Repair of Damaged Steel-Concrete Composite Girders Using Carbon Fiber-Reinforced Polymer Sheets

M. Tavakkolizadeh, A.M.ASCE,[1] and H. Saadatmanesh, M.ASCE[2]

Abstract: The aging infrastructure of the United States requires significant attention for developing new materials and techniques to effectively and economically revive this aging system. Damaged steel-concrete composite girders can be repaired and retrofitted by epoxy bonding carbon fiber-reinforced polymer (CFRP) laminates to the critical areas of tension flanges. This paper presents the results of a study on the behavior of damaged steel-concrete composite girders repaired with CFRP sheets under static loading. A total of three large-scale composite girders made of W355×13.6 A36 steel sections and 75-mm-thick by 910-mm-wide concrete slabs were prepared and tested. One, three, and five layers of CFRP sheet were used to repair the specimen with 25, 50, and 100% loss of the cross-sectional area of their tension flange, respectively. The test results showed that epoxy bonded CFRP sheet could restore the ultimate load-carrying capacity and stiffness of damaged steel-concrete composite girders. Comparison of the experimental and analytical results revealed that the traditional methods of analysis of composite beams were conservative.

DOI: 10.1061/(ASCE)1090-0268(2003)7:4(311)

CE Database subject headings: Rehabilitation; Fiber reinforced polymers; Carbon; Girders; Concrete; Steel; Sheets.

Introduction

Different local and federal agencies have developed programs to rate bridges throughout the United States during the last few decades. Their findings have been alerting to civil engineers nationwide. It has been found that more than one third of the highway bridges in the United States are considered substandard. According to the latest National Bridge Inventory (NBI) update, the number of substandard highway bridges in this country is more than 167,000, more than half of which are structurally deficient (FHWA Bridge Program Group 2001).

Steel bridges comprise more than 34% of the total number of bridges in the United States and were among the most recommended group for improvement based on the NBI report. Many of these bridges need to be repaired due to permanent damage to critically stressed locations of the tension members. These damages were caused by direct physical impact, corrosion, or growth of small cracks under fatigue loading (gradual loss of the cross section). Considering the repair and retrofit option before deciding to replace a bridge is the rational approach. Rehabilitation and repair in most cases is far less costly than replacement. In addition, this usually takes less time, shortening service interruption periods. Because there are limited resources available to mitigate the problems associated with substandard bridges, the need for adopting cost-effective techniques and new materials is apparent.

Fiber-reinforced polymers (FRPs) possess excellent mechanical and physical properties that make them excellent candidates for repair and retrofit of steel girder bridges. FRPs are made of high strength filaments (tensile strength in excess of 2 GPa) such as glass, carbon, and kevlar placed in a resin matrix. Carbon fiber-reinforced polymers (CFRPs) display outstanding mechanical properties, with typical tensile strength and modulus of elasticity of more than 1,200 MPa and 140 GPa, respectively. In addition, the CFRP laminates weigh less than one fifth of the steel and are corrosion resistant.

CFRP plates or sheets can be epoxy bonded to the tension face of the damaged members to restore strength and stiffness. The CFRP sheets bridge over the damaged area and transfer the stresses across. The stress level in the original member will decrease, and that will result in a longer fatigue life. There have been several studies on repair and retrofit of concrete girders with epoxy bonded FRP materials during the past decade; however, very few of them have addressed the use of epoxy bonded composite plates or sheets for strengthening and repair of steel girders.

This paper discusses the effectiveness of epoxy bonding CFRP sheets to the tension flange of damaged steel-concrete composite girders to restore their ultimate load-carrying capacity and stiffness.

Previous Work

The most commonly used techniques for repair of damaged steel bridges include strengthening of damaged members, replacing of members, and adding of members. In general, all of these conventional techniques require heavy machinery and long periods of service interruption, and all are costly. In most cases, they do not eliminate the possibility of reoccurrence of the problem completely.

The most common attachment technique for performing conventional repair is welding. These techniques usually include

[1]Assistant Professor, Dept. of Civil Engineering, Jackson State Univ., Jackson, MS 39217.

[2]Professor, Dept. of Civil Engineering and Engineering Mechanics, The Univ. of Arizona, Tucson, AZ 85721.

Note. Discussion open until April 1, 2004. Separate discussions must be submitted for individual papers. To extend the closing date by one month, a written request must be filed with the ASCE Managing Editor. The manuscript for this paper was submitted for review and possible publication on April 10, 2001; approved on June 25, 2002. This paper is part of the ***Journal of Composites for Construction***, Vol. 7, No. 4, November 1, 2003. ©ASCE, ISSN 1090-0268/2003/4-311–322/$18.00.

welding of a cover plate to the damaged area after performing general clean-up and preventative measures. Unfortunately, welded cover-plates pose several problems, such as the need for heavy machinery, sensitivity of the welded detail to fatigue, and the possibility of galvanic corrosion between the welded plate, existing members, and attachment materials.

The first reported application of epoxy bonding of steel plates for strengthening of concrete structures dates as far back as 1964 in Durban, South Africa, where the reinforcements in a concrete beam were accidentally left out during construction (Dussek 1980). The beam was strengthened by epoxy bonding steel plates to the tension face. By 1975, in Japan, more than 200 defective elevated highway concrete slabs were strengthened with epoxy bonded steel plates (Raithby 1980).

In a study conducted at the University of Maryland, adhesive bonding and end bolting of steel cover plates to the tension flange of steel girders provided a substantial improvement in the fatigue life of the system (Albrecht et al. 1984). They reported an increase in the fatigue life of more than twenty times, as compared to the welded cover plates.

In another study conducted at the University of South Florida, the possibility of using CFRP in the repair of steel-concrete composite bridges was investigated (Sen and Liby 1994). They tested a total of six 6.10-m-long beams made of W203×10.9 steel sections attached to 710-mm-wide by 115-mm-thick concrete slabs. The CFRP sheets used in the study were 3.65 m long, 150 mm wide, and had two different thicknesses of 2 and 5 mm. It was reported that CFRP laminates could considerably improve the ultimate flexural capacity of composite beams.

The advantages of using advanced composite materials in the rehabilitation of deteriorating bridges were investigated at the University of Delaware (Mertz and Gillespie 1996). As a part of their small-scale tests, they retrofitted eight 1.52-m-long W203 ×4.5 steel beams using five different retrofitting schemes. They reported an average of 60% flexural capacity increase in CFRP retrofitted systems. They also tested and repaired two 6.4-m-long corroded steel girders. The girders were typical American Standard I shapes with depths of 610 mm and flange widths of 230 mm. Their results showed an average of 25% increase in stiffness and 100% increase in the ultimate load carrying capacity.

In a study conducted by the writers at The University of Arizona, the effectiveness of CFRP patches for repairing damaged steel beams was investigated (Tavakkolizadeh and Saadatmanesh 2001b). A total of eight small-scale S127×4.5 steel beams were tested. The tension flanges of six beams were cut thoroughly with two different depths of 3.2 and 6.4 mm, then beams were repaired by CFRP patches with different lengths. A four-point bending test was performed using the displacement control loading regime and several unloading and reloading cycles were performed before failure of the beam. In order to avoid lateral instability, the top flanges of the beams were braced using turnbuckle and high strength steel cables at third points and the beam was clamped down at the supports. Increases in ultimate load-carrying capacity of 145% and 63% for the beams with 80% and 40% loss of tension flange area were reported, respectively. The stiffness of the damaged beam after patching was recovered to 95% the original stiffness. The different modes of failures that were observed in the experiments were end peeling and delamination. They indicated that the drawbacks of this technique included the loss of ductility and the possibility of galvanic corrosion between the CFRP plate and steel.

Very few studies have investigated the effectiveness of epoxy bonding CFRP sheets to the tension flange of large-scale steel-concrete composite girders. There is only one study on the effectiveness of this technique for the repair of damaged girders. This study was limited to small-scale steel girders and testing of a couple of corroded large-scale girders.

This paper investigates the effectiveness of epoxy bonding CFRP sheets to tension flange damaged steel-concrete composite girders that lost a portion or their entire tension flange at the most critical location. The experimental results are compared with the conventional methods of analysis. The writers in a separate article have addressed the concern of galvanic corrosion, when CFRP is used in conjunction with steel (Tavakkolizadeh and Saadatmanesh 2001a). The results of this study indicated that galvanic corrosion was not significant and that providing a thin layer of adhesive or a nonmetallic composite layer between the steel and CFRP could further reduce it.

Experimental Study

The feasibility of epoxy bonding of CFRP sheets in restoring the ultimate load-carrying capacity and stiffness of composite girders was examined by testing three large-scale girders repaired with pultruded carbon fiber sheets. In order to observe the effectiveness of this technique, three different damage levels of 25, 50, and 100% loss of tension flange were considered and different thicknesses of CFRP laminates were used. The tension flanges of the girders were cut with different total depths of 43, 86, and 171 mm to simulate 25, 50, and 100% loss of tension flange, respectively. These girders were then strengthened by epoxy bonding of one, three, and five layers of CFRP sheets to the bottom surface of the tension flange. Concrete slabs with two different compressive strengths were used. The overall lengths of CFRP sheets were identical and covered more than over 80% of the girder span. The cut-off points for each layer were staggered to prevent premature failure at termination points due to stress concentrations (Schwartz 1992).

Materials

Tack Coat

A two-component viscous epoxy was used for bonding the laminate to the steel flange surface. The mixing ratio of the epoxy was one part resin (bisphenal A based) to one part hardener (polyethylenepolyamin) by volume. The epoxy had a pot life of 30 min at room temperature and was fully cured after 2 days at 25°C. This epoxy immediately reached high tack consistency and was ideal for over-head applications.

Epoxy

A two-component less viscous epoxy was used for bonding the laminates to each other. The mixing ratio of the epoxy was two parts resin (bisphenal A based) to one part hardener (polyamide) by volume. The epoxy had a pot life of 1 h at room temperature and was fully cured after 7 days at 25°C. This epoxy had a longer gel time and much lower viscosity and was used in between CFRP sheets to insure the least entrapped voids.

CFRP

A unidirectional pultruded carbon fiber sheet with a width of 76 mm and a thickness of 1.27 mm was used. After testing a total of

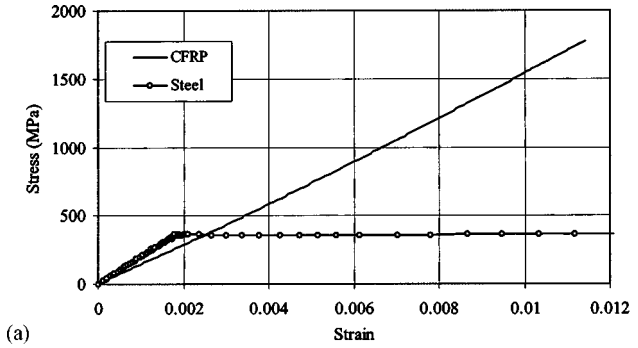

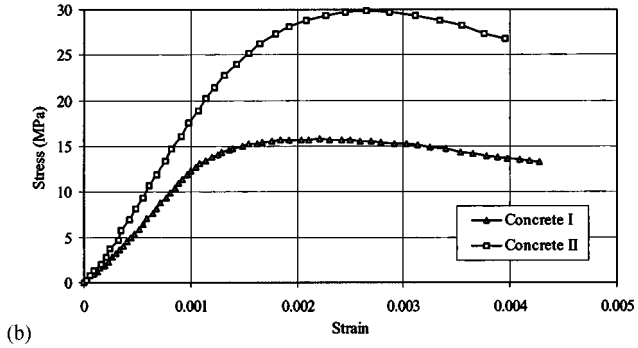

Fig. 1. Typical stress-strain behavior: (a) CFRP and steel; (b) concrete

16 straight strips (coupons) with a length of 400 mm and a width of 25 mm, an average tensile strength of 2,137 MPa, a tensile modulus of elasticity of 144.0 GPa, and a Poisson's ratio of 0.34 were obtained. A typical stress-strain plot for CFRP coupons tested in uniaxial tension is shown in Fig. 1(a).

Steel

W355×13.6 A36 hot rolled sections were used for the experiments. A uniaxial tension test was performed on seven dog-bone specimens with a gauge length of 125 mm, a gauge width of 25 mm, and a thickness of 9.5 and 6.4 mm cut from flanges and the web, respectively. Average yield strengths of 354.9 and 381.9 MPa, moduli of elasticity of 198.3 and 177.5 GPa, and Poisson's ratios of 0.305 and 0.299 were obtained from the specimens cut from the flange and web, respectively. A typical stress-strain plot for the flange in uniaxial tension test is shown in Fig. 1(a). The minimum reinforcement in concrete slabs for temperature and shrinkage was provided by using a 150×150×6.4 mm welded smooth wire mesh.

Concrete

Concrete was ordered from a ready mix plant with nominal compressive strengths of 15.5 and 27.5 MPa, slump of 100 mm, and maximum aggregate size of 10 mm. Twenty 75×150 mm cylinders were made at the time of castings and were kept with the girders during curing. They were tested under uniaxial compression right before the beam tests. The compressive strength and modulus of elasticity of concrete were 16.6 and 29.1 MPa and 13.8 and 19.3 GPa, respectively. Typical stress-strain plots of the concrete with two different compressive strengths under uniaxial compression test are shown in Fig. 1(b).

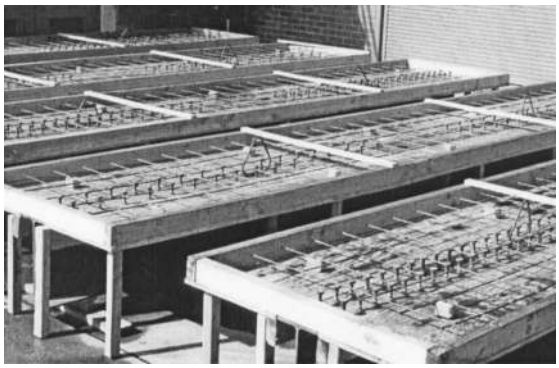

Fig. 2. Formwork for concrete

Specimen Preparation and Instrumentation

The steel sections were first cut into 4.9-m-long beams. Then, shear studs with diameters of 13 mm and heights of 51 mm were welded to the compression flange in two rows 125 mm on center along the two shear spans. After constructing the forms and securing the edges of the forms, the wire mesh was placed in the midheight of the slab by using 38-mm-high chairs, as shown in Fig. 2. Two hooks made of rebar with a diameter of 12.5 mm were welded to the top flange at quarter lengths for transportation of the girders after casting. Slabs (75×910 mm) were cast on two separate times and a hand-held vibrator was used for compaction. Several 75×150 mm cylinders were cast at the same time as the slabs for compression testing. The girders and cylinders were kept moist under a plastic cover for one week.

CFRP sheets were cut to the proper length with a band saw. For the specimen retrofitted with one layer, a pair of 75-mm-wide, 3.95-m-long CFRP sheets was placed side by side and bonded to a 171-mm-wide tension flange. For the specimen retrofitted with three layers, three pairs of CFRP sheets were cut to 3.95, 3.65, and 3.35 m long (150 mm staggers) and placed side by side on the steel girder. For the specimen retrofitted with five layers, CFRP sheets were cut to the lengths of 3.95, 3.80, 3.65, 3.50, and 3.35 m (75 mm staggers). The ends of the sheets were finished smoothly using grid 150 sandpaper. The surfaces of the sheets were sand blasted with No. 30 sand, then washed with saline solution and rinsed with fresh water. After drying of the sheets, for multiple layer systems, the surfaces of the sheets were covered with thick layers of epoxy and were squeezed together to force

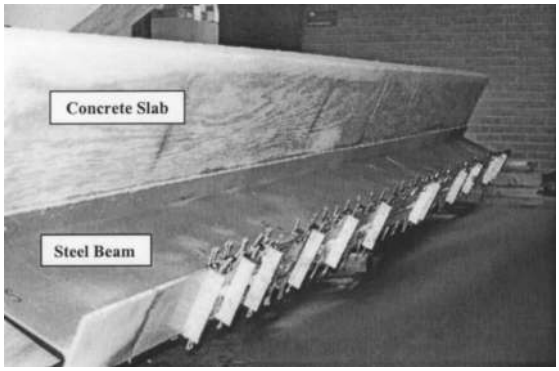

Fig. 3. Endview of typical repaired girder showing binder clips and aluminum angels

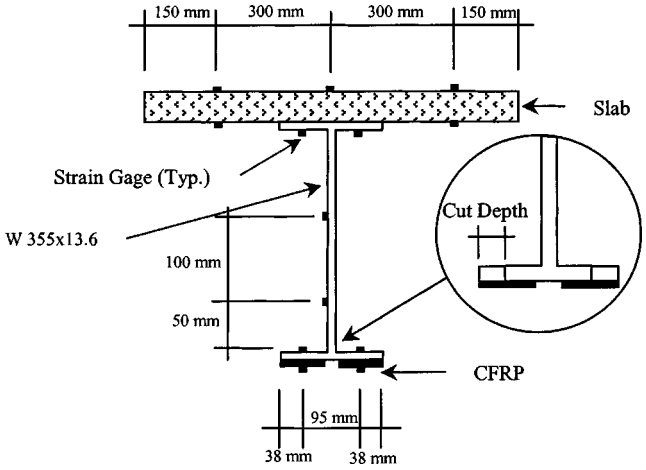

Fig. 4. Schematic of strain gauge locations at midspan

the air bubbles and the excess epoxy out. Binder clips were used in close intervals for securing the edges of the sheets together.

After the concrete slabs were completely cured, the tension flanges of the girders were cut using a Recipro Saw with a 1.27-mm-thick blade. The flanges of the girder with the 15.5 MPa concrete strength were cut 42.7 mm deep on both sides at the midspan (50% loss). The tension flanges of the other two girders with higher concrete compressive strength were cut entirely (100% loss) and 21.4 mm deep on both sides at the midspan (25% loss). Just before applying the CFRP sheets, the tension flange of each girder was sand blasted using No. 30 sand, washed with saline solution, and rinsed with fresh water.

Upon drying of the steel beam and the CFRP sheets, the tack coat was mixed and applied to the tension flange surface and the sheets. The cut at midspan were also filled with adhesive. All pieces were covered with uniform and thin layers of tack coat and were squeezed together to force the air pockets out with excess epoxy. The CFRP sheets were secured throughout their lengths using binder clips and 40×40×3 mm aluminum angle bars, while the tack coat was curing. After two hours, the extra epoxy around the bond area was scraped off. A typical retrofitted specimen is shown in Fig. 3.

After one week, electrical strain gauges with resistance of 120 Ohms were mounted on the surfaces of the steel beam, CFRP sheets, and the concrete slab. In the midspan, the strain gauges were mounted on the top and bottom of the concrete slab, the top

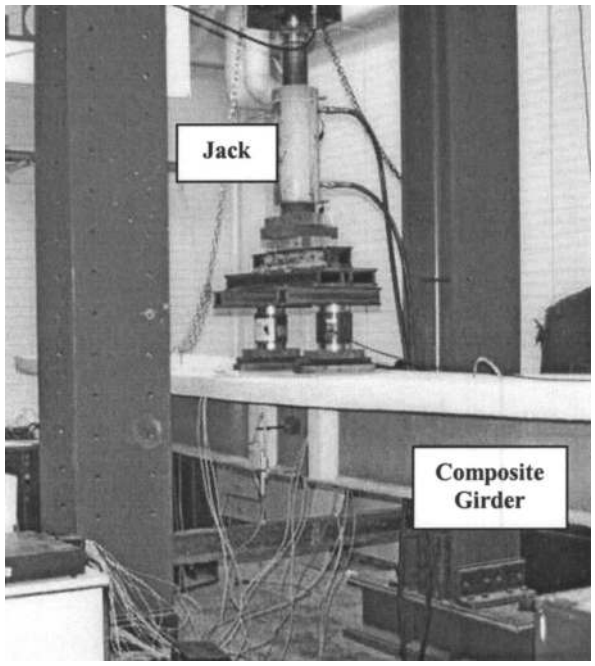

Fig. 6. Test setup

flange and web of the steel beam, and on the CFRP sheets. In addition, strain gauges were mounted at the end and at the quarter-length on the CFRP sheets and the tension flange. The locations of the strain gauges at midspan are shown in Fig. 4.

Eight 100×100 mm wooden blocks were cut and tightly fit between the flanges using cider wedges at the supports and under the loading blocks to prevent web crippling. Two loading platens on top of the slab were prepared by casting two 100×400×5 mm blocks using anchoring cement (Pour-Stone). The blocks were 500 mm apart and placed symmetrically on both sides of the midspan along the center of the slab.

Experimental Setup

Four-point bending tests were performed using a 2,200 kN test frame. Loading was applied by an MTS-244.41 hydraulic actuator and an Enerpac-RRH10011 hydraulic jack with capacities of 500 and 1,000 kN, respectively. The Enerpac had to be used because the capacity of the MTS actuator was limited to 500 kN. The load

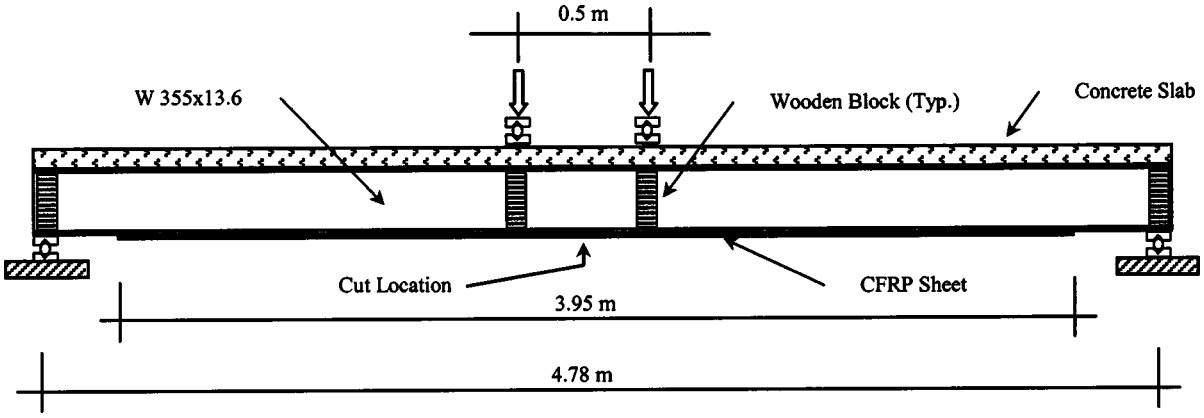

Fig. 5. Schematic of loading setup

Table 1. Constitutive Properties of Materials

Concrete			Steel			CFRP	
Compression	I	II	Tension	Web	Flange	Tension	
Strength (MPa)	16.6	29.1	Yield strength (MPa)	381.9	354.9	Strength (MPa)	2,137
Modulus (GPa)	13.8	19.3	Modulus (GPa)	177.5	198.3	Modulus (GPa)	144.0
Peak strain	0.00197	0.00241	Poisson's ratio	0.299	0.305	Poisson's ratio	0.34
Failure strain	0.00399	0.00352	Strain hardening onset	0.0278	0.0263	Failure strain	0.0148

was measured by two MTS-661.23A-02 load cells with a capacity of 500 kN each and the deflection was measured by a DUNCAN 600 series transducer with a range of ±75 mm. Monotonic loading was performed under actuator displacement control with a rate of 0.025 mm/s. A total of three unloadings were carried out during each test: before steel yielded, after steel yielded, and at 500 kN load level (switching from the actuator to the jack). The load, midspan deflection, and strains at different points were recorded with a Daytronic System 10 data acquisition system interfacing with a PC through Microsoft Excel software.

The clear span was 4.78 m and the loading points were 0.5 m apart, as shown in Fig. 5. The loading points and supports were made using rolling blocks, and one sphere blockhead was used to transfer the load from the hydraulic jack to the spreader beam. The test setup is shown in Fig. 6.

Analytical Modeling

The ultimate strength design method adopted by American Association of State Highway and Transportation Officials (AASHTO) was used to predict the ultimate load-carrying capacity of the damaged and repaired girders. In addition, an incremental deformation method insuring compatibility of deformations and equilibrium of forces was used in the analysis to estimate the moment-curvature behavior of the composite sections. The analytical curves were stopped when the strain in the extreme fiber in the concrete reached 0.0038.

Moment-Curvature Behavior

The moment-curvature behavior of the steel-concrete-CFRP girder was predicted considering the following assumptions:

1. Linear strain variation across the depth of the cross section,
2. Perfect bond between steel, concrete, and CFRP, i.e., perfect composite action and no slippage,
3. Elastic-perfectly-plastic behavior for steel ($\varepsilon<0.025$),
4. Hognestad's parabola for concrete stress-strain relationship (Park and Paulay 1975), and
5. Linear elastic behavior for CFRP.

Uniaxial tension and compression tests were performed on the materials in order to obtain their constitutive properties. The results of these tests are listed in Table 1. The stress-strain plots for the concrete with two different compressive strengths and the corresponding Hognestad's parabolas are shown in Fig. 7.

In order to develop the relationship between the moment and curvature of a section, the concrete slab, top flange, web, and bottom flange were discretized into ten strips each with equal thickness. The CFRP sheet was considered as one layer. The strain at top of the concrete slab was the primary parameter that varied at each step and the depth of the neutral axis was calculated by trial and error. A pair of values for moment and curvature was obtained at each point.

The ultimate compressive strength and strain for concrete were assumed to be 29.1 MPa and 0.38%, respectively. The theoretical moment-curvature plots for the damaged composite girders before retrofitting are shown in Fig. 8. It is apparent that cutting the

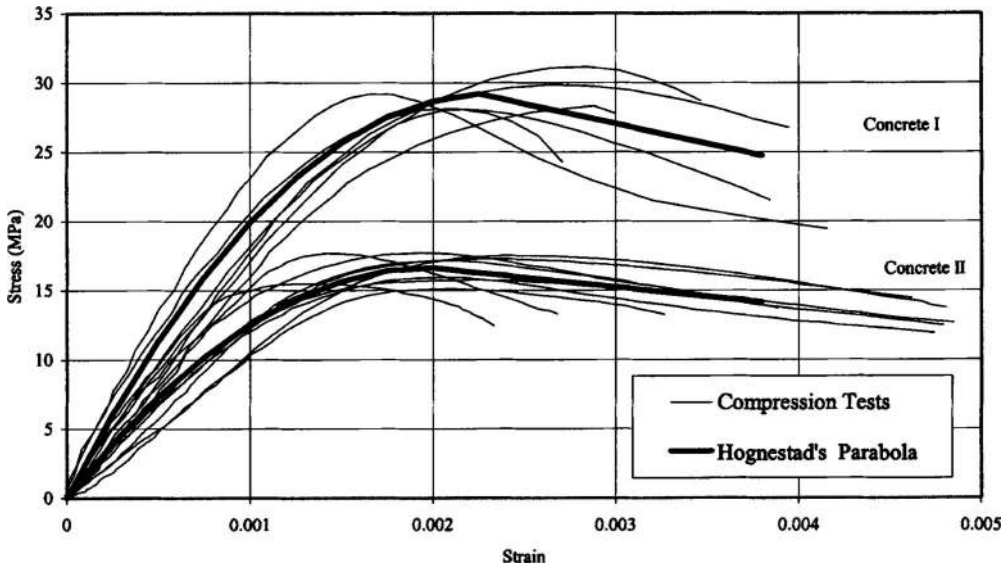

Fig. 7. Constitutive modeling of concrete with different strengths (I: 16.6 MPa; II: 29.1 MPa)

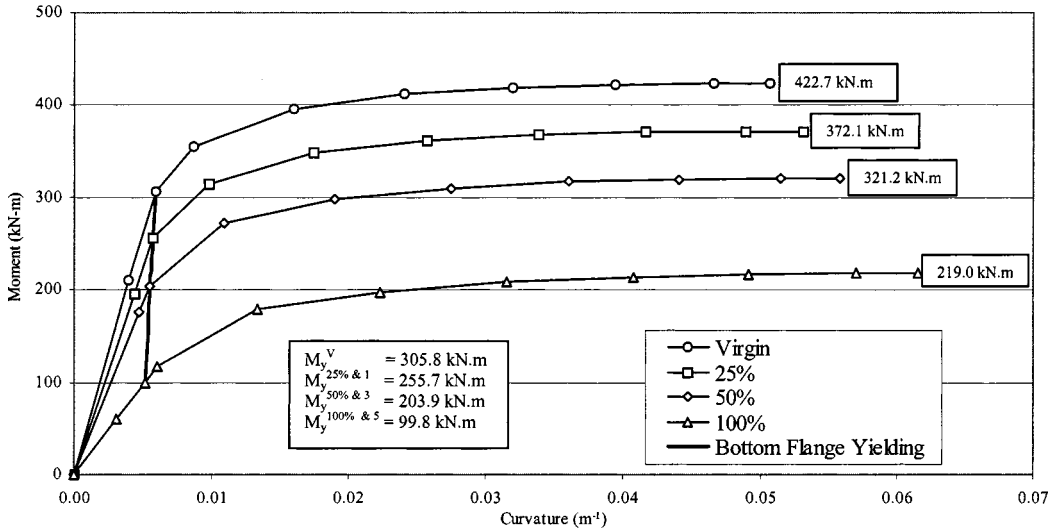

Fig. 8. Theoretical moment-curvature plot for damaged girders

flange reduced the ultimate moment capacity and rigidity of the sections significantly. The ultimate moment capacity of the composite girder reduced 12, 24, and 48% while the yielding moments (moments at the onset of tension flange yielding) decreased by 16, 33, and 67% as a result of 25, 50, and 100% loss of tension flange area, respectively. Meanwhile, the flexural rigidity of sections reduced by 14, 29, and 63% before yielding due to losses of 25, 50, and 100%, respectively. Three damaged sections were then assumed to be retrofitted. CFRP provided additional tension force to overcome the loss of steel flange. The required area of composites was selected such that the tensile stress in the CFRP layers remained between 30 and 35% of their ultimate tensile strength after the tension flange yielded. One, three, and five layers of CFRP sheet were considered for repairing the sections with 25, 50, and 100% tension flange loss, respectively. The ultimate moment capacity and rigidity of the retrofitted sections increased significantly, as shown in Fig. 9. The ultimate moment capacity of the girders with 25, 50, and 100% loss improved by 39, 107, and 233%, while the yielding moment increased by 6, 25, and 85%, respectively. The elastic and postelastic rigidity of the retrofitted sections increased as well. Girders with 25, 50, and 100% loss showed a 5, 21, and 75% increase in their elastic rigidity, respectively. Rigidity in the plastic region (the slope of the linear segment) displayed much higher improvements and increased 6.3, 17.3, and 29.7 times for 25, 50, and 100% loss of tension flange, respectively. A summary of the theoretical values for the ultimate capacity and the rigidity of the sections is listed in Table 2.

Ultimate Moment Capacity (AASHTO)

AASHTO uses the Whitney's block approximation to estimate the compression stress in concrete at failure (AASHTO 1992). In this approach, the ultimate strain in concrete is assumed to be 0.003. Using this method and considering different properties for the web and flanges, the nominal moment capacity and the ultimate curvature of the sections were obtained. The results are shown in Table 3. By adding CFRP sheets to the flange of damaged steel girders, the moment capacity increased significantly and the neutral axis lowered, which reduced the ultimate curvature and duc-

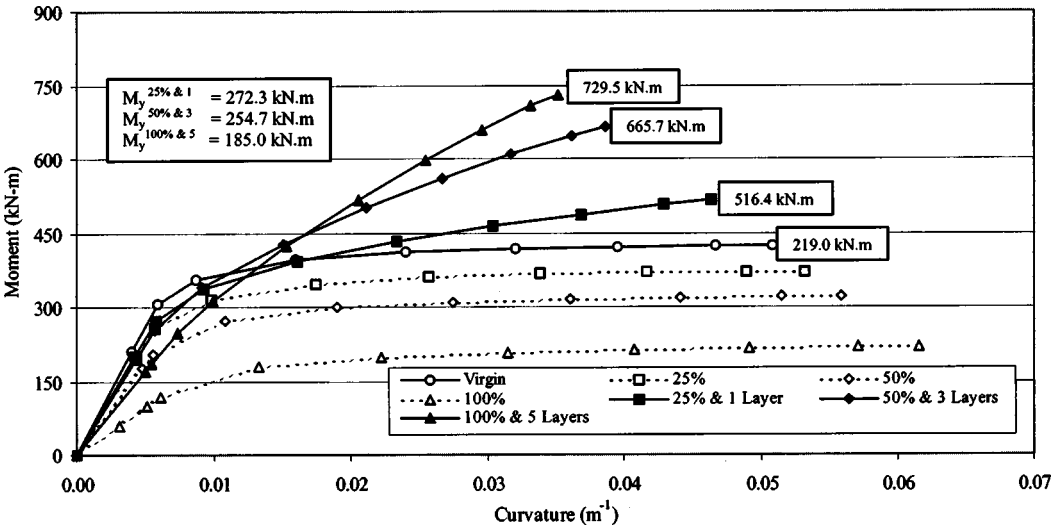

Fig. 9. Theoretical moment-curvature plot for repaired girders

Table 2. Calculated Moment and Rigidity of Virgin, Damaged, and Repaired Sections ($f'_c = 29.1$ MPa)

Damaged					Repaired				
Damage level	Yielding moment (kN.m)	Elastic rigidity ($MN.m^2$)	Ultimate moment (kN.m)	Plastic rigidity ($MN.m^2$)	Number of CFRP layers	Yielding moment (kN.m)	Elastic rigidity ($MN.m^2$)	Ultimate moment (kN.m)	Plastic rigidity ($MN.m^2$)
25%	255.7	44.57	372.1	0.630	1	272.3	46.97	516.4	3.985
50%	203.9	36.78	321.2	0.581	3	254.7	44.43	665.7	10.024
100%	99.8	19.32	219.0	0.519	5	185.0	33.85	729.5	15.395
Virgin	305.8	51.78	422.7	0.699					

tility of the section. The results of the AASHTO method were more conservative as compared with the values obtained by the iterative numerical method.

Experimental Analysis

Three composite girders were tested in the present study. All three girders were repaired by epoxy bonding of one, three, and five layers of CFRP sheets to their tension flanges. They were subjected to monotonic loading with few unloading cycles. The loading was applied under the displacement control regime with the constant rate of 0.025 mm/s. In the elastic region, data were collected at specified load levels, and after yielding, they were collected at specified deflection levels. The specimens were designed for failure under concrete crushing, but other possible modes of failures that could occur were CFRP sheet rupturing, CFRP sheet debonding, flange local buckling, and web crippling.

Girder with 25% Flange Damage, Repaired with One Layer of CFRP Sheets

The load-deflection behavior of the repaired composite girder with 25% loss in the flange area is shown in Fig. 10. The concrete slab had an average compressive strength of 29.1 MPa. The girder showed a fairly linear response to the load from the beginning. During the unloading cycle in the elastic region (not shown), no sign of permanent deformation and nonlinearity was observed. The elastic stiffness of the girder was 19.6 kN/mm. The bottom flange of the girder started to yield at the 166.6 kN load level. The CFRP sheet was under a tensile stress of 170.3 MPa, equal to 8% of its ultimate strength at that point. Proceeding into the postelastic region, the girder was twice unloaded and reloaded. The elastic stiffnesses of the first and second reloading segments were 21.5 and 22.0 kN/mm, respectively. The girder continued to carry the load with a plastic stiffness of 6.7 kN/mm. At the 449.5 kN load level, the CFRP sheet started to show signs of failure (i.e., snapping of the edge fibers) while it was carrying 2,045 MPa, equal to 96% of its tensile strength. The girder failed at 471.8 kN and an ultimate deflection of 49 mm. The ultimate tensile stress in CFRP was 2,298.0 MPa, 7.5% above its average tensile strength. Ultimate compressive strain in the top of the concrete slab reached 0.0018, which is very close to the peak strain value. The sign of extreme deformation at the tip of the cuts was visible and the tension flange at one of the cut tips ruptured 20 mm long, after failure. A few longitudinal cracks were observed in the concrete slab, but they did not have any effect on the result due to their limited width. At the midspan, between two loading points, the web and flanges displayed clear shear plane due to yielding, but there was no buckling and crippling. In other words, the concrete slab and wooden blocks stayed effective in supporting the compression flange and web up to failure. The CFRP sheet tension failure mode was very similar to the one in the uniaxial tension tests. The sheets burst into several narrow and long needle shape pieces attached to the girder at their ends.

Girder with 50% Flange Damage, Repaired with Three Layers of CFRP Sheets

The concrete slab of the second specimen had a compressive strength of 16.6 MPa. The lower strength concrete was used to change the mode of failure to overreinforced compression crushing of concrete. As shown in Fig. 11, the load deflection response of the composite girder was initially linear with a slight curve due to transverse cracks (shrinkage). The stiffness of the girder in the elastic region was 20.4 kN/mm. The unloading and reloading in the elastic region did not show any permanent deformation or hysteresis. The behavior continued to be linear until the tension flange of the girder reached its yielding strain at 136.5 kN. The CFRP sheet was under a small tensile stress of 71 MPa, equal to 3.5% of its strength. At the load level of 245 kN, the epoxy that filled the cut started to separate itself from the steel. Continuing loading of the girder into its postelastic regime, two unloading and reloading cycles were performed at load levels of 400 and 500 kN. While both cycles showed a slight amount of hysteresis, the energy dissipation in the second cycle was more pronounced. The reloading stiffnesses were 20.2 and 18.3 kN/mm for reloading after reaching 400 and 500 kN, respectively. Debonding of the CFRP sheet from the steel girder in the midspan at the cut location (20 mm on each side) started at the load of 480 kN. The

Table 3. Calculated Ultimate Moment and Curvature of Virgin and Repaired Sections ($f'_c = 29.1$ MPa)

Method	Parameter	Virgin	25% loss and one layer	50% loss and three layers	100% loss and five layers
Whitney (AASHTO)	Neutral axis (mm)	98.2	105.4	123.5	128.1
	Moment (kN.m)	393.7	423.2	484.8	501.6
	Curvature (1/m)	0.0305	0.0285	0.0243	0.0234
Hognestad (incremental deformation)	Neutral axis (mm)	74.9	82.0	98.3	108.1
	Moment (kN.m)	422.7	516.4	665.7	729.5
	Curvature (1/m)	0.0507	0.0463	0.0387	0.0351

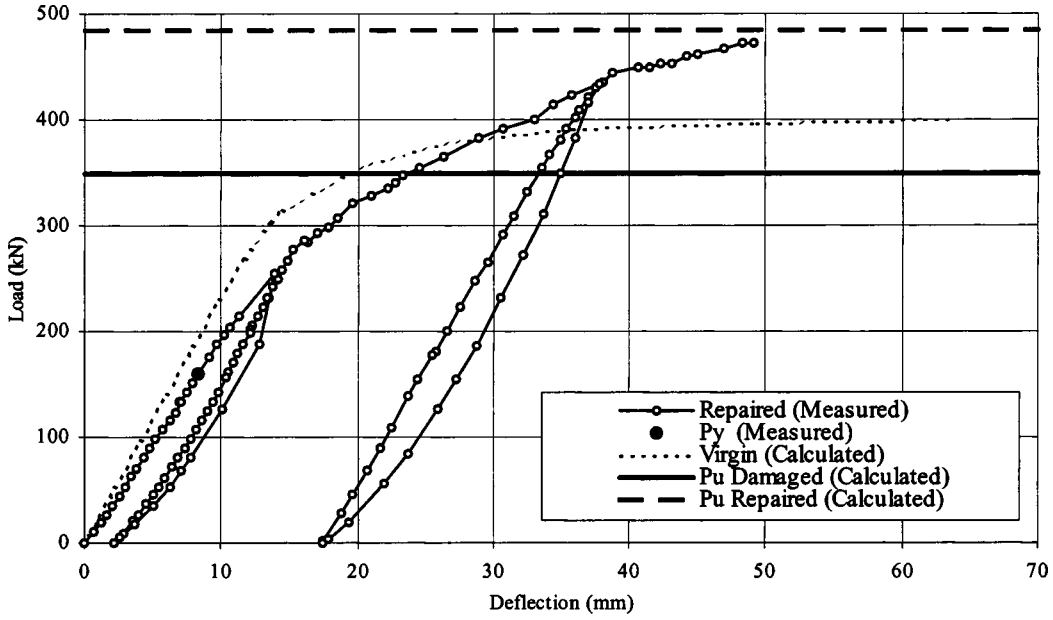

Fig. 10. Load versus deflection of girder with 25% loss in flange area and repaired with one layer of CFRP sheet

lower stiffness in the second and third cycles was due to softening of the concrete and development of longitudinal cracks in the slab, which started to appear at the 475 kN load level. The longitudinal cracks in the slab started to widen at 530 kN and became expanded at 580 kN. The debonding in the midspan grew to 45 and 70 mm on each side of the cut at load levels of 600 and 660 kN, respectively. The concrete slab of the composite girder was almost divided into three longitudinal strips (along the edges of compression flange) at the ultimate load of 658.5 kN, when the girder deflected 74.3 mm. The tensile stress in the CFRP sheet was 1,606 MPa, equivalent to 75% of its strength. The concrete slab was under a strain of 0.0029 and clearly failed in compression. The continuation of the loading was terminated due to buckling and crippling of the compression flange and web after disintegration of the slab. Tensile stress in CFRP sheets went up to 1,748 MPa before termination of the experiment. The concrete failure in compression was the clear mode of failure in this specimen, and the repairing technique clearly recovered the loss of strength and stiffness due to the loss of the tension flange. Overall, the repair technique was successful and the ultimate deflection of the girder was 1.5% of the clear span.

Girder with 100% Flange Damage, Repaired with Five Layers of CFRP Sheets

This specimen was built of the concrete slab with a compressive strength of 29.1 MPa. The complete loss of the tension flange prevented the possibility of measurement of the average tensile

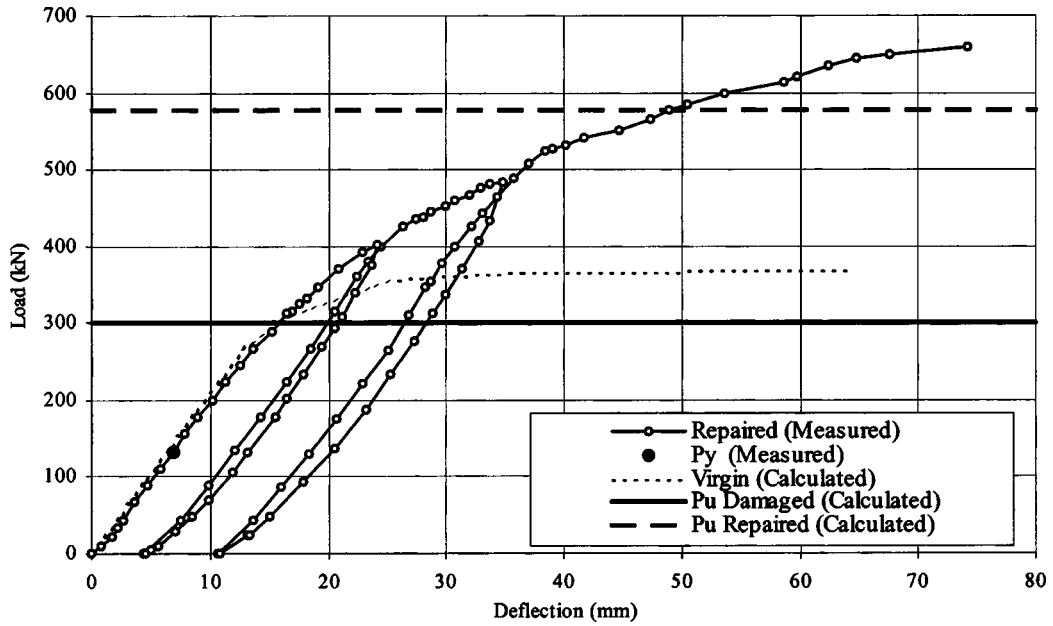

Fig. 11. Load versus deflection of girder with 50% loss in flange area and repaired with three layers of CFRP sheet

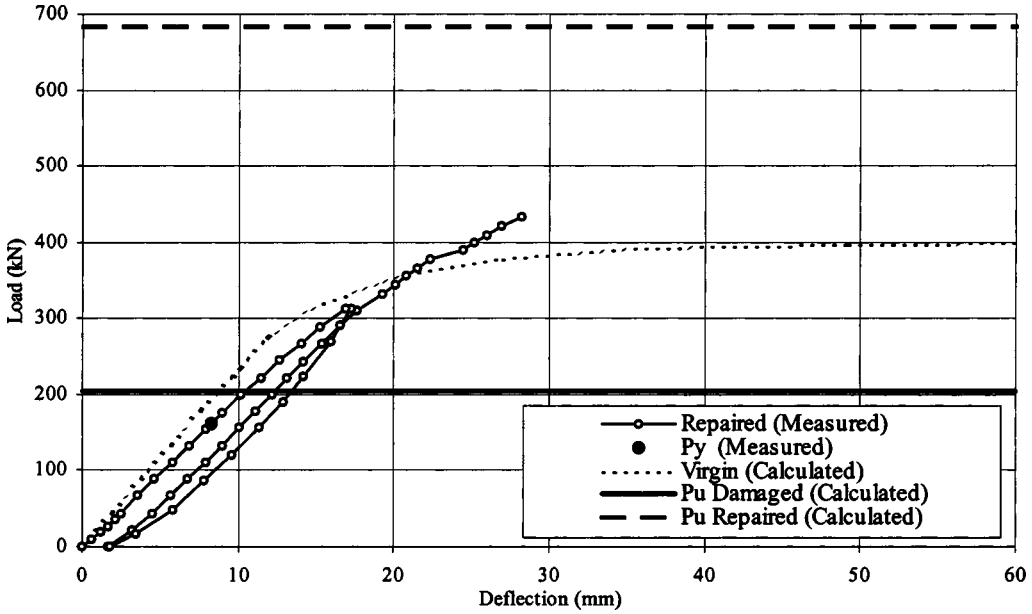

Fig. 12. Load versus deflection of girder with 100% loss in flange area and repaired with five layers of CFRP sheet

strain in the flange directly. Therefore, two strain gauges on the web at midspan were used to obtain hypothetical values of strain in the bottom of the flange. The load-deflection behavior of the repaired girder is shown in Fig. 12. The girder started carrying the load with a fairly linear response. The elastic stiffness of the girder was 19.9 kN/mm and, during the elastic unloading (not shown), there were no signs of permanent deformation or stiffness change. At 133 kN, the epoxy that filled the cut separated from the steel. The linear response continued up to the 162.2 kN load level, at which an extrapolated prediction of the strain at the bottom face of the tension flange reached the yielding strain. The CFRP sheet stress was 194.4 MPa, equal to 9% of its ultimate strength. Continuing loading, the longitudinal cracks appeared at 287 kN and a complete unloading and reloading was performed at 300 kN. There was minimal hysteresis in the loop and the loop closed out at the point that unloading had started. The reloading stiffness was 20.1 kN/mm, very similar to the stiffness at the initial loading. After reaching the load level of 311 kN, the plate started to debond from the steel girder at the cut location in the midspan. Approaching the load level of 380 kN, the failure signs of the CFRP ends were noticed. The girder failed at the load level of 434 kN, due to sudden and complete debonding of the CFRP sheets (initiated from the end) and subsequently rupture of the steel web and failure of the concrete. At the peak load, the CFRP laminate was carrying an 840.1 MPa tensile stress, equal to 40% of its strength, and the concrete strain was 0.0016, well below its failure point. The compression flange and the web did not show any sign of instability due to the support provided by the slab and the wooden blocks in the entire experiment.

Effectiveness of Proposed Technique

Load-Carrying Capacity

After analyzing the experimental results of the composite girders repaired with CFRP sheets, a comparison was made with the theoretical values obtained with the incremental deformation method. The load-carrying capacities of virgin and retrofitted girders were calculated for concrete slab with compressive strengths of 29.1 and 16.6 MPa and tabulated in Table 4. Three repaired girders were able to carry ultimate loads higher than the calculated values for the virgin specimens. The girder with 25% loss and one layer of CFRP displayed a 19.1% increase, while the girder with 100% loss and five layers of CFRP showed a 9.6% increase. The girder with 50% loss and three layers of CFRP, which was made with the concrete slab with lower strength, demonstrated an 80.2% increase.

The predicted capacity of the repaired girders was reasonable. The girder with 25% loss and one layer of CFRP failed at the load of 471.8 kN, fairly close to the predicted value of 484.1 kN (−2.5%). The girder with 50% loss and three layers of CFRP failed after sustaining a load of 658.5 kN. The predicted values for failure of this girder were 578.3 kN, very conservative estimates (+13.8%). The predicted load-carrying capacity of the girder with 100% loss and five layers of CFRP was 683.8 kN. The girder failed at a load of 434.1 kN and a deflection of 2.82 cm due to early debonding of the CFRP sheet. In addition to the peeling stress due to shear concentration, the edges of the large cut tended to deform unevenly during loading and, as a result, high normal peeling stresses were developed at the crack edges, as shown in Fig. 13. This normal stress in addition to the shear stress concentration resulted in progressive debonding that started from the midspan.

Table 4. Calculated and Experimental Load-Carrying Capacity of Virgin and Repaired Girders

Repair techniques (concrete strength)	Measured (kN)	Calculated (kN)	Virgin calculated (kN)
25% loss and one layer ($f'_c = 29.1$ MPa)	471.8	484.1	396.2
50% loss and three layers ($f'_c = 16.6$ MPa)	658.5	578.3	365.4
100% loss and five layers ($f'_c = 29.1$ MPa)	434.0	683.5	396.2

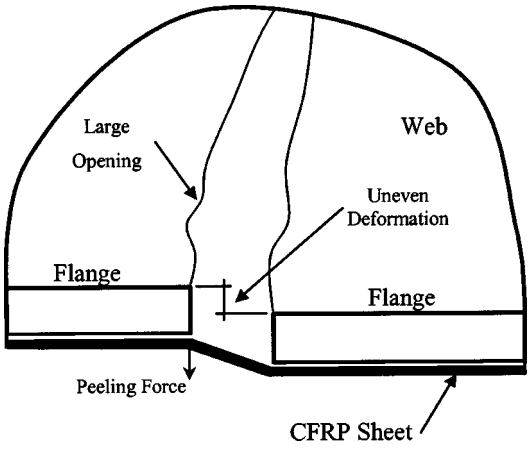

Fig. 13. Schematic of peeling mechanism at large crack opening

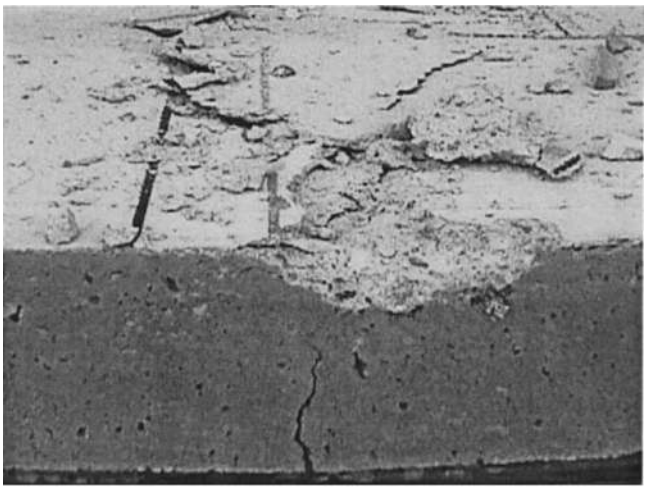

(a)

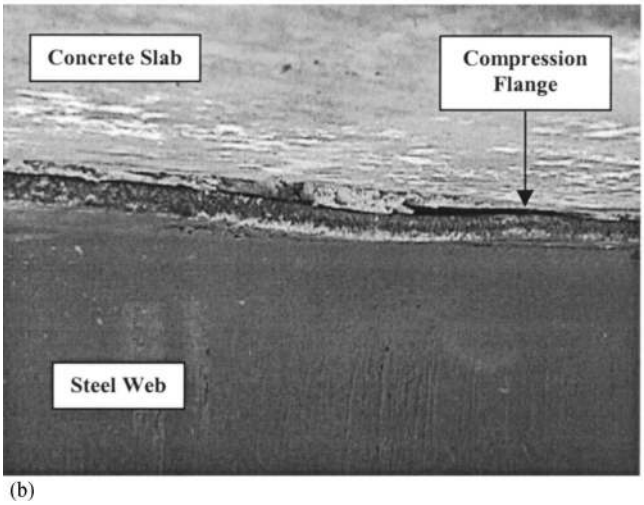

(b)

Fig. 14. Failure due to compression crushing: (a) concrete crushing; (b) flange instability

Elastic and Postelastic Stiffnesses

The predicted value for the elastic stiffnesses of the virgin composite girders made with 29.1 MPa compressive strength concrete was 23.1 kN/mm. The repair technique was not able to recover the loss of the stiffness completely for the two girders with higher compressive strength concrete. The average stiffnesses of the girders were 21.0 (−8.9%) and 20.0 kN/mm (−13.5%) for 25 and 100% loss of flange, respectively. The repaired girder with a lower compressive strength (50% loss) recovered its lost stiffness due to the damage completely and displayed a stiffness of 196.7 kN/cm, compared to the predicted value of 19.2 kN/mm (+2.4%). Table 5 summarizes the experimental and theoretical values of the stiffnesses of the virgin and repaired girders.

Failure Modes

As indicated previously, the steel-concrete-CFRP system could display several distinct failure modes, including concrete crushing, CFRP debonding, CFRP rupture, flange buckling, web crippling, and shear stud failure. The wooden blocks placed between the flanges at the supports and under loading points prevented web crippling. Shear stud failure was avoided by designing the shear studs for a concrete slab with 35 MPa compressive strength, well above the strength of the concrete used in this study.

Crushing of concrete, as shown in Fig. 14(a), was the dominating failure mode for the girder made of 16.6 MPa concrete. The three-layer repair system for a girder with a 50% loss of its tension flange forced the slab to carry the maximum compressive strain of beyond 0.29% before failure. Meanwhile, the extent of damage to the slab and the widening of longitudinal cracks after failure allowed the flange and web to buckle, as shown in Fig. 14(b). The progressive debonding of the CFRP sheet was limited to a short length of less than 150 mm at both sides of the cut in the midspan.

The tension rupture of CFRP sheets, as shown in Fig. 15(a), was the distinct mode of failure for the composite girder with 25% loss of tension flange area that was repaired with one layer of CFRP sheet. There was no sign of debonding or concrete compression failure. The slab supported the compression flange and prevented buckling despite developing a few longitudinal cracks along the edges of the compression flange. The rupture of the CFRP sheet was sudden and there was no sign of bond failure between the CFRP sheet and the steel flange. The concrete slab barely reached its peak strength and experienced a compressive strain of 0.18% at the time of failure. The steel flange at the tip of the cuts showed cracking at the base of the cut as shown in Fig. 15(b).

Failure of the bond between the CFRP laminate and steel flange was the mode of failure in the girder with 100% loss of tension flange, repaired with five layers of CFRP sheets. Failure progressed quickly from the first sign of debonding at the cut in the midspan (72% of failure load) to the progressive sign of debonding at the end of the sheets (88% of failure load) and eventually complete failure, as shown in Fig. 16(a). The bond between

Table 5. Calculated and Experimental Stiffnesses of Virgin and Repaired Girders

	Measured stiffness (kN/mm)		Calculated stiffness (virgin) (kN/mm)	
Repair techniques	Elastic	Postelastic	Elastic	Postelastic
25% loss and one layer	21.0	6.7	23.1	0.3
50% loss and three layers	19.7	4.6	19.2	0.2
100% loss and five layers	20.0	10.1	23.1	0.3

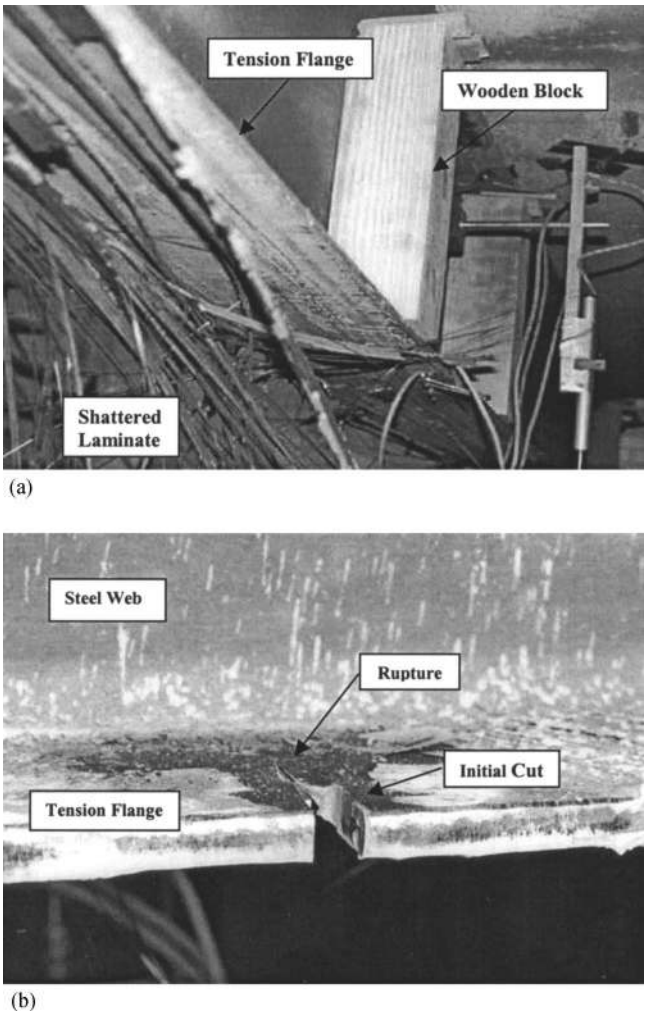

Fig. 15. Failure due to CFRP rupture: (a) ruptured sheet; (b) flange rupture at tip of cut

the sheet and the steel girder failed and the impact of sudden failure forced delamination between the layers. The web of the girder ruptured at the same time as the CFRP sheets debonded, as shown in Fig. 16(b). The compressive strain in the concrete was 0.16%, well below its capacity. There were no signs of longitudinal cracking in the slab up to failure point. The shear planes in the web and flange were very pronounced, as shown in Fig. 16(c).

Conclusions

Test results for repair of damaged steel-concrete composite girders by epoxy bonding of CFRP laminates to the damaged area are very promising. For all three damage levels of 25, 50, and 100% considered in this study, this technique improved the ultimate load-carrying capacity well beyond that of the virgin girder. The effect of CFRP laminates on the stiffness was also notable. Based on the results of the experimental investigation, the following conclusions are drawn:

1. Ultimate load-carrying capacities of the girders significantly increased by 20, 80, and 10% for the 25% damaged and one-layer, 50% damaged and three-layer, and 100% damaged and five-layer repairing systems.
2. The effect of CFRP bonding on the elastic stiffness of the girders was significant. The technique restored the elastic stiffness of the girder to 91, 102, and 86% of the intact girder for the 25% loss and one-layer, 50% loss and three-layer, and 100% loss and five-layer repairing systems.
3. The effect of the technique on improving the postelastic stiffness of the repaired girder was much more pronounced. The stiffness was increased 21, 19, and 32 times as compared with the intact girder.
4. The analytical models using the Hognestad's parabola provided an accurate estimate in the case of CFRP rupture and

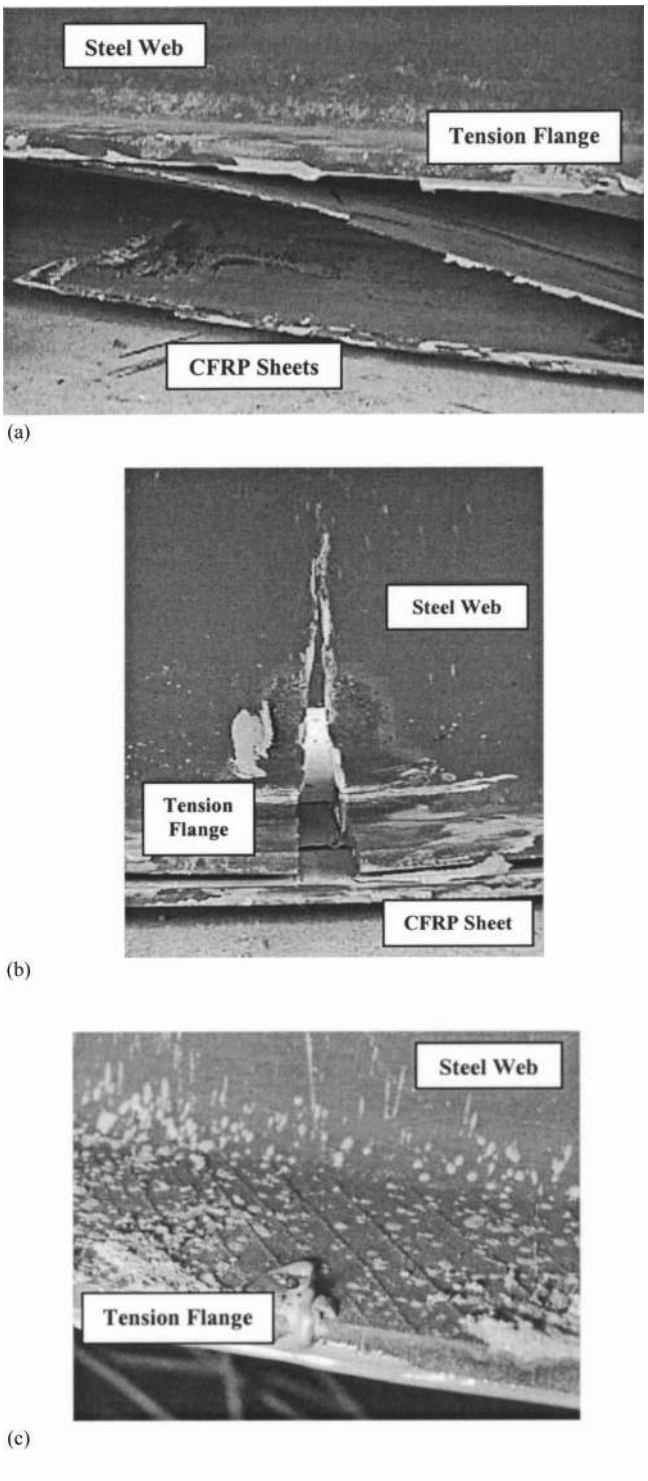

Fig. 16. Failure due to debonding: (a) CFRP sheets debonding; (b) web rupture; (c) shear planes

small loss in tension flange area. For the mode of failure due to compression crushing of concrete and moderate loss of tension flange area, the theory was fairly conservative. For significant loss of tension flange and in order to consider the debonding mode of failure, the stress concentration and peeling stresses at the crack should be considered as the primary cause of failure.

5. While the analytical models indicated that the ductility of the retrofitted system was less than for virgin girders, repaired girders with small to moderate loss of their tension flange deflected between 50 and 75 mm, which is about 1/100 and 1/65 of the clear span.
6. A theoretical model for prediction of debonding of the CFRP sheets needs to be developed in order to consider the possibility of premature failure due to this phenomenon.

Acknowledgments

The writers wish to acknowledge the funding of this research by the National Science Foundation, Grant No. CMS-9413857, Dr. John B. Scalzi, Program Director. The results and conclusions presented here are those of the writers and do not represent the views of the National Science Foundation.

References

Albrecht, P., Sahli, A., Crute, D., Albrecht, Ph., and Evans, B. (1984). ''Application of adhesive to steel bridges.'' *Rep. FHWA-RD-84-037*, Federal Highway Administration, Washington, D.C., 106–147.

American Association of State Highway and Transportation Officials (AASHTO). (1992). *Standard specifications for highway bridges*, 15th Ed., Washington, D.C.

Dussek, I. (1980). ''Strengthening of the bridge beams and similar structures by means of epoxy-resin-bonded external reinforcement.'' *Transportation Research Record 785*, Transportation Research Board, Washington, D.C., 21–24.

Federal Highway Administration (FHWA) Bridge Program Group. (2001). ''Count of deficient highway bridges.'' ⟨http://www.fhwa.dot.gov/bridge⟩.

Mertz, D., and Gillespie, J. (1996). ''Rehabilitation of steel bridge girders through the application of advanced composite material.'' *NCHRP Rep. 93-ID11*, Transportation Research Board, Washington, D.C., 1–20.

Park, P., and Paulay, T. (1975). *Reinforced concrete structures*, 1st Ed., Wiley, New York.

Raithby, K. (1980). ''External strengthening of concrete bridges with bonded steel plates.'' *Supplementary Rep. 612*, Transport and Road Research Laboratory, Dept. of Environment, Crowthorn, U.K., 16–18.

Schwartz, M. (1992). *Composite material handbook*, 2nd Ed., McGraw-Hill, New York.

Sen, R., and Liby, L. (1994). ''Repair of steel composite bridge sections using carbon fiber reinforced plastic laminates.'' *Rep. FDOT-510616*, Florida Department of Transportation, Tallahassee, Fla.

Tavakkolizadeh, M., and Saadatmanesh, H. (2001a). ''Galvanic corrosion of carbon and steel in aggressive environments.'' *J. Compos. Constr.,* 5(3), 200–210.

Tavakkolizadeh, M., and Saadatmanesh, H. (2001b). ''Repair of cracked steel girder using CFRP sheet.'' *Creative systems in structural and construction engineering*, Balkema, Rotterdam, The Netherlands, 461–466.